Detailed Kinetics and Mechanism of the Oxidation of Thiocyanate Ion (SCN−) by Peroxomonosulfate Ion (HSO_5^-). Formation and Subsequent Oxidation of Hypothiocyanite Ion (OSCN−)

ARTICLE *in* INORGANIC CHEMISTRY · JANUARY 2013

Impact Factor: 4.76 · DOI: 10.1021/ic302544y · Source: PubMed

3 AUTHORS, INCLUDING:

József Kalmár
University of Debrecen
14 PUBLICATIONS **75** CITATIONS
SEE PROFILE

István Fábián
University of Debrecen
120 PUBLICATIONS **1,650** CITATIONS
SEE PROFILE

Inorganic Chemistry

Article

pubs.acs.org/IC

Detailed Kinetics and Mechanism of the Oxidation of Thiocyanate Ion (SCN^-) by Peroxomonosulfate Ion (HSO_5^-). Formation and Subsequent Oxidation of Hypothiocyanite Ion ($OSCN^-$)

József Kalmár,* Gábor Lente, and István Fábián

Department of Inorganic and Analytical Chemistry, University of Debrecen, P.O. Box 21, Debrecen H-4010, Hungary

Supporting Information

ABSTRACT: The haloperoxidase-catalyzed in vivo oxidation of thiocyanate ion (SCN^-) by H_2O_2 is important for generation of the antimicrobial hypothiocyanite ion ($OSCN^-$), which is also susceptible to oxidation by strong in vivo oxidizing agents (i.e., H_2O_2, OCl^-, OBr^-). We report a detailed mechanistic investigation on the multistep oxidation of excess SCN^- with peroxomonosulfate ion (HSO_5^- in the form of Oxone) in the range from pH 6.5 to 13.5. $OSCN^-$ was detected to be the intermediate of this reaction under the above conditions, and a kinetic model is proposed. Furthermore, by kinetic separation of the consecutive reaction steps, the rate constant of the direct oxidation of $OSCN^-$ by HSO_5^- was determined: $k_2 = (1.6 \pm 0.1) \times 10^2\ M^{-1}\ s^{-1}$ at pH 13.5 and $k_2^H = (3.3 \pm 0.1) \times 10^3\ M^{-1}\ s^{-1}$ at pH 6.89. A critical evaluation of the estimated activation parameters of the elementary steps revealed that the oxidations of SCN^- as well as the consecutive $OSCN^-$ by HSO_5^- are more likely to proceed via $2e^-$-transfer steps rather than $1e^-$ transfer.

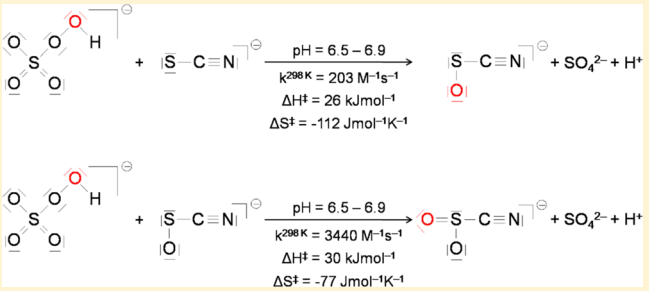

INTRODUCTION

The diverse, and often catalytic oxidation reactions of thiocyanate anion (SCN^-) are intensively studied (vide infra) because the biological importance of this anion is connected to its vivid in vivo redox chemistry.[1] In addition, SCN^- is an environmental pollutant, and its oxidative removal from industrial wastewater is essential. Furthermore, the in situ oxidation of SCN^- is of fundamental importance during thiocyanation of various compounds in synthetic organic chemistry.

Thiocyanate ion is enzymatically oxidized by H_2O_2 to the antimicrobial hypothiocyanite ion[2] ($OSCN^-$) in vivo.[3−5] The rate of the direct $SCN^- + H_2O_2$ reaction is slow,[6] but defensive peroxidase enzymes found in neutrophils (myeloperoxidase[7]) and eosinophil granulocites (eosinophil peroxidase[8]) catalyze this reaction effectively. Extracellular enzymes in milk (lactoperoxidase[9]), in airways (lactoperoxidase[10]), and in saliva (salivary peroxidase[11]) are also efficient catalysts for the oxidation of SCN^- by H_2O_2. Furthermore, $OSCN^-$ is a potent bactericide and plays an important role in multiple stages of the nonimmune defense system[3,4] at several physiological locations (e.g., in the mouth[12] and in airways[13,14]). Thus, the insufficiently low in vivo local concentration of its precursor SCN^- is assumed to play an important role in the development of several chronic diseases, like cystic fibrosis.[1,15] SCN^- can be oxidized to $OSCN^-$ in a noncatalytic way by hypochlorous acid (HOCl)[16] and by hypobromous acid (HOBr).[17] These reactions may be important in controlling the redox activities of those defensive peroxidase systems where $SCN^-/OSCN^-$ and Cl^-/OCl^- or Br^-/OBr^- are simultaneously present. The understanding of the in vivo redox chemistry of SCN^- is further complicated by the fact that the $2e^-$ oxidation product of SCN^-, $OSCN^-$, can be subsequently oxidized by the same oxidizing agents as SCN^-, i.e., H_2O_2, HOCl, or HOBr.[3−5] The reactions of $OSCN^-$ with these oxidizing agents are difficult to study because $OSCN^-$ cannot be synthesized in the absence of excess SCN^-. This problem is attributed to the "overoxidation" of $OSCN^-$, which is assumed to be of a similar order of magnitude as its production from SCN^-.[3,5,18] The half-life of the decomposition of $OSCN^-$ is on the order of several minutes at pH 7,[19] further limiting the applicable experimental conditions.

From environmental aspects, SCN^- and cyanide ion (CN^-) are considered to be the main inorganic anionic pollutants of wastewater and recycled water from metallurgical, mostly gold extraction plants. Although the toxicity of CN^- is undoubtedly higher than that of SCN^-, the latter can be found in larger quantities in metallurgical wastewater and is more toxic to fish. The removal of SCN^- is important for the detoxification of industrial water because molecular oxygen can oxidize SCN^- to sulfate (SO_4^{2-}) and CN^- on a longer time scale, especially under UV radiation. For this reason, the admissible limit of SCN^- in metallurgical wastewater is usually as low as 0.05 mg/L. Technologically feasible processes for SCN^- removal almost exclusively utilize oxidative degradation approaches.[20] The

Received: November 20, 2012
Published: January 30, 2013

   dx.doi.org/10.1021/ic302544y | Inorg. Chem. 2013, 52, 2150−2156

fundamental reactions of these processes are catalytic,[21−23] photocatalytic,[24,25] and also biological oxidations.[26,27] The universal goal is to convert SCN^- quantitatively into environmentally more tolerable cyanate ion (OCN^-) [or carbonate ion (CO_3^{2-}) and nitrogen (N_2)] and SO_4^{2-}. The oxidizing agents of choice are usually hydrogen peroxide (H_2O_2)[21] and ozone (O_3)[23] in order to avoid the formation of any hazardous side products.

The oxidation of SCN^- plays a crucial role in organic synthetic strategies aiming at the preparation of thiocyanated compounds. To create a reactive intermediate for thiocyanation of both aromatic[28−30] and aliphatic[31−33] compounds, a mixture of various oxidizing agents is used in situ with thiocyanate salts. Some of these synthetic methods utilize HSO_5^- in the form of Oxone as the oxidizing agent in order to achieve milder reaction conditions with higher yields.[30,32,33]

HSO_5^- is a peroxo compound and resembles H_2O_2 in its redox behavior, although the reactions of HSO_5^- with inorganic reducing agents[34,35] are characteristically faster than those of H_2O_2. The oxygen-transfer reactions of HSO_5^- to halide ions (Cl^-, Br^-, and I^-) are described in detail.[34] Stoichiometric[36] and kinetic results[37,38] indicate that the oxidation of SCN^- by HSO_5^- is a complicated multistep process under acidic conditions, from pH 2.2 to 6.3. The end products were identified as OCN^-, CN^-, and SO_4^{2-}.[36] On the basis of calculations by the initial rate method and using numerical integration for simulating kinetic observations, Smith and Wilson concluded that the key initial step in the overall reaction is the equilibrium (R0H) between SCN^- and HSO_5^-,[37,38] where "HOSCN" is an uncharacterized intermediate.

$$HSO_5^- + SCN^- \rightleftharpoons SO_4^{2-} + HOSCN \qquad \text{(R0H)}$$

The formation of a second intermediate [thiocyanogen: $(SCN)_2$] is proposed in the rapid comproportionation of SCN^- and HOSCN, which inhibits accumulation of HOSCN under acidic conditions. This comproportionation is well characterized in the literature.[19,39] In our present study, the kinetics and mechanism of the oxidation of SCN^- by HSO_5^- are characterized in a wide range of pH values from the physiologically relevant neutral to the highly basic, where the comproportionation of SCN^- + $OSCN^-$ to give $(SCN)_2$ is negligible;[19] thus, $OSCN^-$ accumulates.

EXPERIMENTAL SECTION

Reagents and Solutions. NaSCN (99.99+ %) and Oxone were purchased from Sigma-Aldrich and used without further purification. The $KHSO_5$ content of Oxone was regularly checked by iodometric titration. All other chemicals were purchased in the highest available purity and used without further purification. Ultrafiltered (Milli-Q, Millipore) water was used for preparing solutions. The pH of the reaction mixture was maintained either by phosphate buffer (from pH 6.5 to 7.8), by borate buffer (from pH 8.0 to 10), or by NaOH (from pH 11 to 13). The pH was measured by a Metrohm 6.0234.110 combined glass electrode attached to a Metrohm 721 NET Titrino titrating unit. The electrode was calibrated by two buffers according to IUPAC recommendations.[40] The ionic strength was adjusted by $NaClO_4$.

Kinetic Measurements. Fast kinetic experiments were carried out in an Applied Photophysics DX-17 MV stopped-flow instrument with either a photomultiplier tube or a photodiode array installed as the detector. Absorbance traces were collected using an optical cell of 10.0 mm path length. The dead time of the stopped-flow instrument was determined by the reaction of 2,6-dichlorophenol−indophenol with ascorbic acid (AA) under pseudo-first-order conditions with AA in excess.[41] The dead time of the instrument was measured to be 1.51 ± 0.03 ms, allowing determination of the first-order rate constants (k_{obs}) up to 500 s^{-1}. The temperature was maintained within ±0.1 °C during all stopped-flow measurements with a Julabo F-12 refrigerated/heated circulator.

Electrospray Ionization Mass Spectrometry (ESI-MS). ESI-MS measurements were performed with a Bruker micrOTOF$_Q$ mass spectrometer equipped with a quadrupole and time-of-flight (Q-TOF) analyzer. The detailed description of the methodology is given in our recent study.[19] The aim of the MS experiments was to identify the intermediates and products of the HSO_5^- + SCN^- reaction in a quick and sensitive, but qualitative way.

Software. The raw data sets of the measurements were processed with instrument-controlling software. Typically, *Micromath Scientist 2.0*[42] was used for Levenberg−Marquard least-squares fitting procedures. Multiple sets of kinetic curves recorded under different initial conditions were simultaneously evaluated with the program package *ZiTa*[43] using the *GEAR* algorithm.[44]

RESULTS AND DISCUSSION

Oxidation of SCN^- with HSO_5^- in the Range from pH 7 to 13. For the sake of simplicity, we studied the reaction of HSO_5^- with SCN^- at pH 13.5 first, where HSO_5^- is fully deprotonated [$pK_a(HSO_5^-)$ = 8.35 at I = 1.0 M[34]], and hypothiocyanite ($OSCN^-$), the expected product of an oxygen transfer to SCN^-, is stable for hours.[45] The reaction was studied under high excess of SCN^- ($[SCN^-]_0$ = 50.0−500 mM) over SO_5^{2-} ($[HSO_5^-]_0$ = 5.0 mM). The reaction is complete in a few seconds under the conditions applied, and additional kinetic effects were not observed on longer time scales. Kinetic traces were recorded at various wavelengths in the range of 350−500 nm (Figure 1) and analyzed by singular-

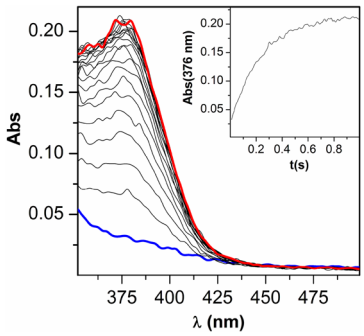

Figure 1. UV−vis spectral change recorded in the SO_5^{2-} + SCN^- reaction system at pH 13.5. The absorbance maximum at 376 nm is characteristic of $OSCN^-$. The first (blue) and last (red) spectra are highlighted. Inset: Kinetic curve recorded at 376 nm. $[KHSO_5]_0$ = 5.0 mM; $[NaSCN]_0$ = 500 mM; pH 13.5; I = 1.0 M; T = 25.0 °C.

value decomposition analysis (Table S1 in the Supporting Information) in order to determine the number of absorbing species in the system.[46,47] It was found that the increase in absorbance during the reaction at around 375 nm can be attributed to the formation of a single species; no absorbing intermediates were detected. The observed product was unambiguously identified as $OSCN^-$ with an absorbance maximum at 376 nm.[48] $OSCN^-$ was also identified with an ESI-MS method (see the Supporting Information) described in our recent study.[19] In subsequent experiments, the kinetic curves were exclusively recorded at 376 nm, where neither the reactants nor other products contribute to the absorbance. All kinetic traces (Figure 2, right panel) could be fitted with a single-exponential function within the precision of the experimental data (R^2 > 0.98) and show the following

dx.doi.org/10.1021/ic302544y | Inorg. Chem. 2013, 52, 2150−2156

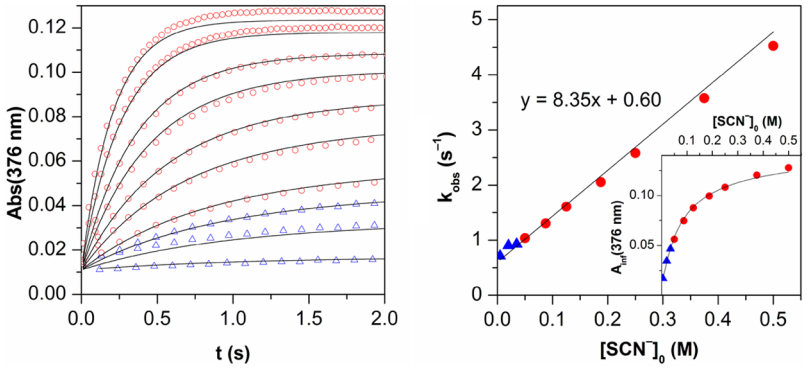

Figure 2. Reaction of SCN^- with SO_5^{2-} at pH 13.5. Left panel: experimental pseudo-first-order kinetic curves; only 5% of the recorded points are shown for clarity. Right panel: pseudo-first-order rate constant as a function of the initial SCN^- concentration. Inset: Final absorbance at 376 nm as a function of the initial SCN^- concentration. The symbols are the same for the two panels. Circles: experimental points with SCN^- in high excess. Triangles: comparable $[SCN^-]_0$ and $[SO_5^{2-}]_0$. Lines: result of a global fit to the kinetic model of Scheme 1. $[KHSO_5]_0$ = 5.0 mM; $[NaSCN]_0$ = 5.0–500 mM; pH 13.5; I = 1.0 M; T = 25.0 °C.

characteristics: the final absorbance readings reach a limiting value by increasing $[SCN^-]_0$, and the experimental pseudo-first-order rate constant (k_{obs}) is linearly dependent on $[SCN^-]_0$ with a nonzero intercept (Figure 2, left panel).

At high SCN^- excess, $OSCN^-$ is produced following a 1:1 $OSCN^-$-to-SO_5^{2-} stoichiometry. From the highest final absorbance, $[OSCN^-]_{max}$ = 5.1 mM was calculated using the literature value of the molar absorbance of $OSCN^-$ at 376 nm (26.5 M^{-1} cm^{-1}).[48] Phenomenologically, such observations can be explained by an equilibrium reaction between the reactants (R0), which is pseudo-first-order in both directions[49] (these conditions are fulfilled because SCN^- and SO_4^{2-} are in large excess[50] over the limiting reagents):

$$SO_5^{2-} + SCN^- \rightleftharpoons SO_4^{2-} + OSCN^- \quad \text{(R0)}$$

A similar equilibrium (R0H) was proposed previously in the kinetic model of the reaction of SCN^- + HSO_5^- under acidic conditions.[37,38] However, considering that the backward reaction of R0 is hardly feasible thermodynamically[51] and that the kinetics of the SO_5^{2-} + SCN^- reaction system proved to be indifferent to the change in $[SO_4^{2-}]_0$ (Figure S1 in the Supporting Information), the existence of equilibrium R0 was ruled out. An alternative kinetic model was constructed, keeping in mind that the rate of oxidation of $OSCN^-$ by peroxo compounds is expected to be about the same order of magnitude as the rate of oxidation of SCN^-.[3,5,18] In the kinetic model shown in Scheme 1, SCN^- and its first-step oxidation product $OSCN^-$ are competing for the remaining SO_5^{2-} in reactions R1 and R2, respectively. With an increasing excess of SCN^-, the relative rate of the oxidation of $OSCN^-$ decreases; thus, the surviving amount of $OSCN^-$ increases. The stoichiometry of the production of $OSCN^-$ becomes 1:1 ($OSCN^-$-to-SO_5^{2-}) at high $[SCN^-]_0$. The oxidation product of $OSCN^-$ (i.e., O_2SCN^-) is known to decompose in fast reactions (R3–R6, adopted from the literature[39,52]) to yield the final mixture of stable anions: SO_4^{2-}, SO_3^{2-}, CN^-, and OCN^-.[19,39,52] The production of SO_4^{2-}, CN^-, and OCN^- is observed during the oxidation of SCN^- by HSO_5^- at acidic pH.[36] The formation of SO_3^{2-} is detected during the decomposition of $OSCN^-$ at neutral pH.[19] The presence of CN^- and OCN^- in the basic SCN^- + SO_5^{2-} reaction mixture was verified by ESI-MS in this study (see the Supporting Information) with a method detailed earlier.[19] The experimental kinetic data set recorded at pH 13.5 was fitted globally

Scheme 1. Kinetic Model for the Oxidation of SCN^- by SO_5^{2-} at around pH 13[a]

$$SO_5^{2-} + SCN^- \rightarrow SO_4^{2-} + OSCN^- \qquad k_1 \qquad \text{(R1)}$$

$$SO_5^{2-} + OSCN^- \rightarrow SO_4^{2-} + O_2SCN^- \qquad k_2 \qquad \text{(R2)}$$

$$2\,O_2SCN^- \rightarrow O_3SCN^- + OSCN^- \qquad \textit{(R3)}$$

$$O_2SCN^- + OSCN^- \rightarrow O_3SCN^- + SCN^- \qquad \textit{(R4)}$$

$$O_3SCN^- + 2\,OH^- \rightarrow SO_4^{2-} + CN^- + H_2O \qquad \textit{(R5)}$$

$$O_3SCN^- + 2\,OH^- \rightarrow SO_3^{2-} + OCN^- + H_2O \qquad \textit{(R6)}$$

[a]Although $k_1 \ll k_2$, at high concentrations of SCN^-, the first oxidation step (R1) can compete with the faster second step (R2); thus, $OSCN^-$ can accumulate. Reaction steps *R3*, *R4*, *R5*, and *R6* in italics are adopted from the literature[52,39] and assumed to be much faster than R1 and R2.

to the two-step kinetic model utilizing the *ZiTa* software package and assuming that both the R1 and R2 steps are first-order for each species involved. The actual rates of reactions R3 and R4 were considered to be comparable and much faster than those of the rate-determining steps (R1 and R2) over the entire course of the reaction, thus not affecting the stoichiometry of the depletion of $OSCN^-$. The fit was excellent even at comparable initial concentrations of SCN^- and SO_5^{2-} (Figure 2). The calculated rate constants are k_1 = 8.08 ± 0.02 M^{-1} s^{-1} and k_2 = 164.8 ± 0.5 M^{-1} s^{-1}.

A derivation on the basis of the system of simultaneous differential equations defined by Scheme 1 yields the following approximate expression for the concentration change of $OSCN^-$ as a function of time (see the Supporting Information):

$$[OSCN^-] = \frac{k_1[SCN^-][SO_5^{2-}]_0}{k_1[SCN^-] + k_2[SO_5^{2-}]_0} \times \{1 - \exp[-(k_1[SCN^-] + k_2[SO_5^{2-}]_0)t]\} \quad (1)$$

Although the derivation shows that Scheme 1 does not predict a simple first-order kinetic trace in a strict mathematical sense, eq 1 implies that the actual solution is close to an exponential curve with a pseudo-first-order rate constant $k_{obs} = k_2[HSO_5^-]_0 + k_1[SCN^-]_0$. This explains why the kinetic traces could be fitted to a simple first-order expression with reasonable

dx.doi.org/10.1021/ic302544y | Inorg. Chem. 2013, 52, 2150–2156

accuracy. The k_{obs} versus $[SCN^-]_0$ plot in Figure 2 (right panel) can be fitted to $k_{obs} = m[SCN^-]_0 + a$ acceptably, yielding $m = 8.351 \pm 0.001$ M^{-1} s^{-1} and $a = 0.601 \pm 0.001$ s^{-1} at constant $[SO_5^{2-}]_0 = 5.0$ mM. A comparison with eq 1 gives $k_1 = 8.35$ M^{-1} s^{-1} and $k_2 = 120$ M^{-1} s^{-1}. These rate constants are in good agreement with those estimated by globally fitting the experimental data set to the kinetic model of Scheme 1 without approximations. These results lend further support to the kinetic model proposed in Scheme 1.

The title reaction was also studied in detail at pH 6.89, where the protonated form of the oxidant, HSO_5^-, is predominant over SO_5^{2-}, but $OSCN^-$ is still deprotonated [pK_a(HOSCN) = 4.93 at $I = 1.0$ M[19]]. In the first 100 ms after mixing the reactants, the kinetic behavior of the reaction is similar to that observed at pH 13.5 (Figures 3 and S2 in the Supporting Information). Thus, the findings can be interpreted using the kinetic model of Scheme 1 by replacing SO_5^{2-} with HSO_5^-:

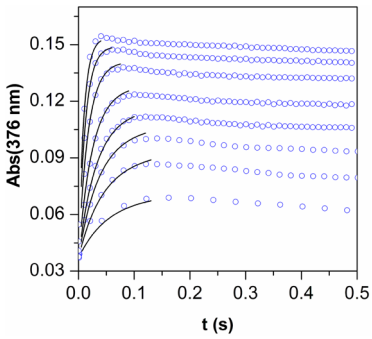

Figure 3. Experimental kinetic curves recorded in the reaction of SCN^- + HSO_5^- at pH 6.89. Two kinetically separated phases are shown (a third slower step is not included in the figure). The faster process can be described with the kinetic model of Scheme 1. Open circles: experimental curves. Only 5% of the recorded points are shown for clarity. Lines: results of the global fit of the first part of the kinetic traces to the kinetic model of Scheme 1. $[KHSO_5]_0 = 5.0$ mM; $[NaSCN]_0 = 25-500$ mM; pH 6.89; $I = 1.0$ M; $T = 25.0$ °C.

$$HSO_5^- + SCN^- \rightarrow SO_4^{2-} + OSCN^- + H^+ \qquad k_1^H \quad \text{(R1H)}$$

$$HSO_5^- + OSCN^- \rightarrow SO_4^{2-} + O_2SCN^- + H^+ \qquad k_2^H \quad \text{(R2H)}$$

The values of the rate constants were estimated by globally fitting the first part of the kinetic curves with *ZiTa*: $k_1^H = 203 \pm 1$ M^{-1} s^{-1} and $k_2^H = (3.44 \pm 0.03) \times 10^3$ M^{-1} s^{-1} (Figures 3 and S2 in the Supporting Information). On a longer time scale (>100 ms), two additional kinetically independent reaction steps were observed. The second process (Figure 3) is characterized by a small decrease in the absorbance at 376 nm in a few seconds, and according to the matrix rank analysis of the multivawelength measurements, it does not involve the formation of any new absorbing species (Table S1 in the Supporting Information). A semiquantitative observation was made that the amplitude of the absorbance change during the second process significantly decreases with increasing $[SCN^-]_0$ and even vanishes at high $[SCN^-]_0$. This phenomenon makes the quantitative description of this reaction step challenging but, on the other hand, leads to the assumption that the second process is probably attributed to the reaction of $OSCN^-$ with CN^-:

$$CN^- + OSCN^- \rightarrow \rightarrow OCN^- + SCN^- \qquad \text{(R7)}$$

CN^- is formed in reaction R5 (Scheme 1) after the oxidation of $OSCN^-$ by HSO_5^- (R2H). With increasing $[SCN^-]_0$, the produced amount of CN^- decreases as the relative rate of oxidation of $OSCN^-$ (R2H) decreases. Similar observations were made previously regarding the role of CN^- in the reaction system of SCN^- + HSO_5^- at highly acidic pH.[36,37] The CN^- + $OSCN^-$ reaction (R7) was already investigated in detail in a wide range of pH values by directly mixing the two reactants[53] and is known to be reasonably fast only at pH < 7, which explains the absence of this process in the SO_5^{2-} + SCN^- reaction system at pH 13.5. The inclusion of R7 in the kinetic model of Scheme 1 is not necessary because the SCN^- + HSO_5^- and $OSCN^-$ + CN^- reactions are kinetically independent in the applied pH range. The third and slowest process observed at pH 6.89 resulted in the complete depletion of $OSCN^-$ in minutes. This last and slowest process was identified as the hydrolytic decomposition of $OSCN^-$ to give simple inorganic anions such as CN^-, OCN^-, SO_4^{2-}, and SO_3^{2-}, which were already described in our earlier work.[19]

The pH dependence of the $(H)SO_5^-$ + SCN^- reaction was studied in the range from pH 6.9 to 13.5. The useful pH range was limited because HOSCN rapidly decomposes at 2 < pH < 6[19] and HOSCN and SCN^- rapidly comproportionate to give $(SCN)_2$ at pH < 2.[39] In order to determine the apparent rate constants for the oxidation of both SCN^- (k_1^{app}) and $OSCN^-$ (k_2^{app}) at a given pH, the kinetic experiments were run in duplicate at two different $[SCN^-]_0$ values. The two rate constants were computed by simultaneously fitting these pairs of experimental kinetic curves to the kinetic model of Scheme 1. The values of both k_1^{app} and k_2^{app} decrease in a sigmoidal fashion with increasing pH, as seen in Figure 4. An excellent description of these pH profiles can be given by taking into account the reactivity difference between HSO_5^- and SO_5^{2-}:

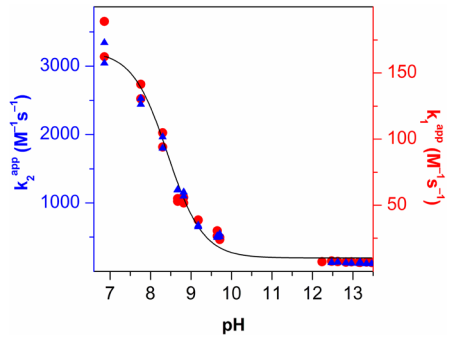

Figure 4. pH dependence of the SCN^- + $(H)SO_5^-$ reaction system. Closed circles (right *y* scale): apparent rate constants for the oxidation of SCN^- with $(H)SO_5^-$. Triangles (left *y* scale): apparent rate constants for the oxidation of $OSCN^-$ with $(H)SO_5^-$. Line: result of a simultaneous fit to eqs 2 and 3. The *y* scales are normalized to each other. $[KHSO_5]_0 = 5.0$ mM; $[NaSCN]_0 = 50.0$ or 500 mM; $I = 1.0$ M; $T = 25.0$ °C.

$$k_1^{app} = k_1^H \frac{[H^+]}{K_a + [H^+]} + k_1 \frac{K_a}{K_a + [H^+]} \qquad (2)$$

$$k_2^{app} = k_2^H \frac{[H^+]}{K_a + [H^+]} + k_2 \frac{K_a}{K_a + [H^+]} \qquad (3)$$

dx.doi.org/10.1021/ic302544y | *Inorg. Chem.* 2013, 52, 2150−2156

where K_a is the acid dissociation constant of HSO_5^- and rate constants k_1, k_1^H, k_2, and k_2^H are defined in previous paragraphs. In the final calculations, all kinetic traces recorded at various reactant concentrations and pH values were fitted simultaneously to the kinetic model of Scheme 1, taking into account the pH dependence of the system. These estimated values for k_1, k_1^H, k_2, and k_2^H are listed in Table 1. The excellent fit between

Table 1. Calculated Rate Constants and Activation Parameters in the Reaction System $(H)SO_5^-$ + SCN^-

reaction	studied at pH	$k^{298\ K}$ ($M^{-1}\ s^{-1}$)	$\Delta H^{\ddagger}$ (kJ mol^{-1})	$\Delta S^{\ddagger}$ (J $mol^{-1}\ K^{-1}$)
R1	13.5	$(1.0 \pm 0.2) \times 10^1$	35.2 ± 0.5	−108 ± 2
R2	13.5	$(1.6 \pm 0.1) \times 10^2$		
R1H	6.9	$(2.0 \pm 0.2) \times 10^2$	26 ± 1	−112 ± 3
R2H	6.9	$(3.3 \pm 0.1) \times 10^3$	30 ± 2	−77 ± 5

the experimental results and the calculated data is illustrated in Figure 4. The estimate for $pK_a(HSO_5^-)$ = 8.43 ± 0.05 (I = 1.0 M) is in good agreement with previously published values.[34] The apparent rate constants k_1^{app} and k_2^{app} were found to decrease linearly with decreasing $[H^+]$ in the range from pH 12.3 to 13.5 (Figure S3 in the Supporting Information), where $[H^+] \ll K_a(HSO_5^-)$ and both eqs 2 and 3 are simplified to linear correlations. This observation, together with the results of the full-scale pH-dependence study, is strong evidence against the presence of any acid/base-catalyzed processes in the $(H)SO_5^-$ + SCN^- reaction system.

The temperature dependence of the HSO_5^- + SCN^- reaction was studied in phosphate buffer at pH 6.54 (measured at 25.0 °C), where the rates of the reactions R1 and R2 are negligible compared to those of R1H and R2H, respectively. The pH was chosen to be far (at least 1.5 units away) from the pK_a values of both HSO_5^- and HOSCN at 25.0 °C, and phosphate buffer was chosen because its pH shows less than a −0.05 unit/+10 K dependence on the temperature.[54] Thus, all complications arising from the possible temperature-dependent shifting of the protolytic equilibria in the reaction system were averted by carefully choosing the experimental conditions. In order to obtain information on the temperature dependence of the rate of reactions R1H (k_1^H) and R2H (k_2^H), the same approach as that in the pH-dependence study was used: two duplicate kinetic experiments were run at two different $[SCN^-]_0$ values at a given temperature. The calculated rate constants k_1^H and k_2^H are shown in Figure 5 in the temperature range from 5.0 to 45.0 °C. Because both R1H and R2H are elementary reactions, the Eyring equation was used to calculate the activation parameters by utilizing a nonlinear least-squares fitting algorithm:[55]

$$k = \frac{k_b T}{h} \exp\left(\frac{\Delta S^{\ddagger}}{R}\right) \exp\left(-\frac{\Delta H^{\ddagger}}{RT}\right) \quad (4)$$

where k_b is the Boltzmann constant, h is the Planck constant, R is the universal gas constant, and $\Delta S^{\ddagger}$ and $\Delta H^{\ddagger}$ are the activation entropy and enthalpy. The resulting activation parameters are listed in Table 1. The temperature dependence of the oxidation of SCN^- with SO_5^{2-} (R1) was also studied at pH 13.5. The excess of SCN^- used in these kinetic experiments ($[SO_5^{2-}]_0$ = 5.0 mM and $[SCN^-]_0$ = 750 mM) was chosen to be high to avoid the oxidation of $OSCN^-$ by SO_5^{2-} (R2). In other words, the rate of reaction R2 was negligible compared to R1 under the applied experimental conditions, and k_1 could be

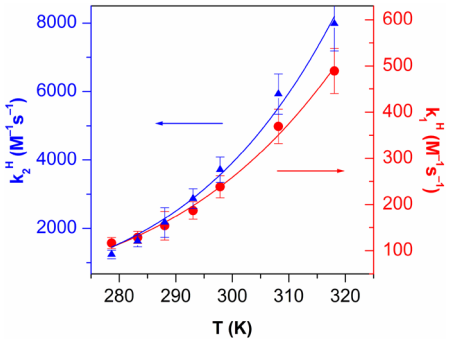

Figure 5. Temperature dependence of the reaction between SCN^- and HSO_5^- at pH 6.54. Circles (right y scale): rate constant of the oxidation of SCN^- with HSO_5^- (R1H). Triangles (left y scale): rate constant of the oxidation of $OSCN^-$ with HSO_5^- (R2H). Lines: results of nonlinear fits to the Eyring equation. $[KHSO_5]_0$ = 5.0 mM; $[NaSCN]_0$ = 50.0 or 500 mM; I = 1.0 M; pH 6.54 (measured at 25.0 °C).

measured directly. With this approach, we lost the possibility of determining the activation parameters of R2 but excluded the possibility of any systematic error arising from the complicated simultaneous evaluation of two sets of kinetic data. The Eyring equation was used again to evaluate the activation parameters from the temperature-dependent study (Figure S4 in the Supporting Information), and the results are listed in Table 1. The entropies of activation of reactions R1H, R1, and also R2H are large negative values close to −100 J $mol^{-1}\ K^{-1}$. Similar entropies of activation were measured in the reactions of HSO_5^- with halide ions (Cl^-, Br^-, and I^-).[34] The analogy between the oxidation of halides and SCN^- is not surprising, taking into account the well-established classification of SCN^- as a pseudohalide ion. With the methodology presented in ref 34, one can conclude that the rate-determining step in the HSO_5^- + SCN^- (R1H) elementary reaction cannot be a $1e^-$-transfer step. At pH 7, the formal potential of the $HSO_5^-/SO4^{\bullet-}$ couple is (1.19 + 0.0591 × log 10^{-7}) = 0.78 V,[34] whereas the standard reduction potential of the $SCN^{\bullet}/SCN^-$ couple is 1.63 V.[56] Thus, the free energy of the possible $1e^-$ HSO_5^- + SCN^- (R1H) elementary step would be [(1.63 − 0.78) × 96.485] = 82 kJ mol^{-1}, which is much higher than the measured free energy of activation at 298 K: (26 + 298 × 0.112) = 59 kJ mol^{-1}. Therefore, similarly to the reactions of halides, the HSO_5^- + SCN^- (R1H) elementary step is more likely to proceed through an initial $2e^-$ oxidation, probably involving concerted heterolytic O−O bond cleavage and S−O bond formation. This mechanism is expected to involve much more geometric reorganization and characterized by higher activation entropy than a $1e^-$-transfer rate-determining step, which does not include atom transfer before the transition state. In accordance with the concluding thoughts of ref 34, a generalization is risky without a sufficiently high number of reliably measured activation parameters in the literature for the reactions of HSO_5^- and SO_5^{2-}. Still the −80 to −110 J $mol^{-1}\ K^{-1}$ activation entropies of R1H, R1, and R2H seem to suggest that all of these processes proceed through $2e^-$-transfer rate-determining steps rather than $1e^-$-transfer steps.

CONCLUSIONS

We showed that peroxomonosulfate ion (HSO_5^-) oxidizes thiocyanate ion (SCN^-) to hypothiocyanite ion ($OSCN^-$) in the range from pH 6.9 to 13.5 (k_1^H = 2.0 × 10^2 $M^{-1}\ s^{-1}$ at pH

dx.doi.org/10.1021/ic302544y | Inorg. Chem. 2013, 52, 2150−2156

6.89). The oxidation of $OSCN^-$ by HSO_5^- ($k_2^H = 3.3 \times 10^3\ M^{-1}\ s^{-1}$ at pH 6.89) also takes place in the reaction system of HSO_5^- + SCN^-. On the basis of the estimated activation parameters, we concluded that the rate-determining steps in the above oxidation processes are more likely to be $2e^-$- than $1e^-$-transfer steps. Because the rate constant of the oxidation of $OSCN^-$ is an order of magnitude higher than that of SCN^-, these two compounds compete for the oxidant HSO_5^-, and the quantitative conversion of SCN^- to $OSCN^-$ is possible only by minimizing the relative rate of the "overoxidation" reaction, using at least a 100-fold excess of SCN^- over HSO_5^-. We derived a simple kinetic model valid under neutral and basic conditions in the SCN^- + HSO_5^- reaction system and showed that the inclusion of the equilibrium step between SCN^- + HSO_5^- and $OSCN^-$ + SO_4^{2-} presented in the Smith and Wilson model[36−38] is not necessary under these conditions. This paper presents quantitative information on the kinetics of the oxidation of antimicrobial $OSCN^-$ by a peroxo compound, which seems to have no precedent in the literature. If the relative reactivities of SCN^- and $OSCN^-$ are expected to be similar toward HSO_5^- and H_2O_2, it is reasonable to assume that the in vivo accumulation of $OSCN^-$ during the defensive peroxidase-catalyzed SCN^- + H_2O_2 reaction is limited by the presence of H_2O_2 itself.

The high rate of the HSO_5^- + SCN^- reaction might make Oxone an attractive choice for technologies aiming at the oxidative removal of SCN^- from metallurgical wastewater, keeping in mind that method optimization is required to completely avoid the formation of toxic CN^- as a product.

We assume that, during the oxidative thiocyanation of aromatic and aliphatic compounds, the in situ formation of protonated HOSCN (hypothiocyanous acid) takes place in the fast reaction of HSO_5^- + SCN^-. In this case, the SCN moiety may act as an S-electrophile reagent because the high electronegativity of the oxygen atom significantly lowers the electron density of the soft sulfur atom. By the protonation of HOSCN to H_2OSCN^+, even the formation of ^+SCN is predictable after water elimination. The formation of an electrophile during the in situ oxidation of SCN^- can account for the success of this polarity inversion (*umpolung*) thiocyanation strategy among activated aromatic and α-acidic oxo compounds.

■ ASSOCIATED CONTENT

Supporting Information

Detailed kinetic and UV−vis spectroscopic information on the oxidation of thiocyanate, results of singular-value decomposition calculations, and deduction of the rate law for the kinetic model of Scheme 1. This material is available free of charge via the Internet at http://pubs.acs.org.

■ AUTHOR INFORMATION

Corresponding Author

*E-mail: kalmar.jozsef@science.unideb.hu.

Notes

The authors declare no competing financial interest.

■ ACKNOWLEDGMENTS

The authors are grateful to Prof. Michael T. Ashby (University of Oklahoma) for critically reading the manuscript. The assistance of Bernadett Biri (University of Debrecen) with the MS measurements and the contribution of Orsolya Molnár to the kinetic measurements are greatly acknowledged. The authors are thankful for the Hungarian Scientific Research Fund [OTKA: K68668 and T49044 (IN64289)], TAMOP 4.2.1./B-09/1/KONV-2010-007, and 4.2.2-08/12 CHEMIKUT. I.F. is grateful for support by the Hungarian Academy of Sciences through the Research Group of Homogeneous Catalysis and Reaction Kinetics.

■ REFERENCES

(1) Xu, Y.; Szép, S.; Lu, Z. *Proc. Natl. Acad. Sci. U.S.A.* **2009**, *106*, 20515−20519.
(2) $OSCN^-$ is derived from HOSCN known commonly as hypothiocyanous acid. The systematic (IUPAC) names of $OSCN^-$ and HOSCN are oxidothiocyanate and hydrogenoxidothiocyanate, respectively.
(3) Hawkins, C. L. *Free Radical Res.* **2009**, *43*, 1147−1158.
(4) Barrett, T. J.; Hawkins, C. L. *Chem. Res. Toxicol.* **2012**, *25*, 263−273.
(5) Ashby, M. T. *Adv. Inorg. Chem.* **2012**, *64*, 263−303.
(6) Figlar, J. N.; Stanbury, D. M. *Inorg. Chem.* **2000**, *39*, 5089−5094.
(7) Kettle, A. J.; Winterbourn, C. C. *Redox Rep.* **1997**, *3*, 3−15.
(8) Wang, J.; Slungaard, A. *Arch. Biochem. Biophys.* **2006**, *445*, 256−260.
(9) Shin, K.; Tomita, M.; Lönnerdal, B. *J. Nutr. Biochem.* **2000**, *11*, 94−102.
(10) Bjorck, L.; Rosen, C. G.; Marshall, V.; Reiter, B. *J. Appl. Microbiol.* **1975**, *30*, 199−204.
(11) Ihalin, R.; Loimaranta, V.; Tenovuo, J. *Arch. Biochem. Biophys.* **2006**, *445*, 261−268.
(12) Ashby, M. T. *J. Dent. Res.* **2008**, *87*, 900−914.
(13) Wijkstrom-Frei, C.; El-Chemaly, S.; Ali-Rachedi, R.; Gerson, C.; Cobas, M. A.; Forteza, R.; Salathe, M.; Conner, G. E. *Am. J. Res. Cell Mol.* **2003**, *29*, 206−212.
(14) Rada, B.; Leto, T. L. *Immunol. Res.* **2009**, *43*, 198−209.
(15) Lorentzen, D.; Durairaj, L.; Pezzulo, A. A.; Nakano, Y.; Launspach, J.; Stoltz, D. A.; Zamba, G.; McCray, P. B., Jr.; Zabner, J.; Welsh, M. J.; Nauseef, W. M.; Bánfi, B. *Free Radical Biol. Med.* **2011**, *50*, 1144−1150.
(16) Ashby, M. T.; Carlson, A. C.; Scott, M. J. *J. Am. Chem. Soc.* **2004**, *126*, 15976−15977.
(17) Nagy, P.; Beal, J. L.; Ashby, M. T. *Chem. Res. Toxicol.* **2006**, *19*, 587−593.
(18) Aune, T. M.; Thomas, E. L. *Eur. J. Biochem.* **1977**, *80*, 209−214.
(19) Kalmár, J.; Woldegiorgis, K. L.; Biri, B.; Ashby, M. T. *J. Am. Chem. Soc.* **2011**, *133*, 19911−19921.
(20) Botz, M. M.; Mudder, T. I.; Akcil, A. U. *Dev. Miner. Process.* **2005**, *15*, 672−702.
(21) Batoeva, A. A.; Tsybikova, B. A.; Ryazantsev, A. A. *Russ. J. Appl. Chem.* **2010**, *83*, 993−996.
(22) Collado, S.; Laca, A.; Díaz, M. *J. Hazard. Mater.* **2010**, *177*, 183−189.
(23) Udrea, I.; Avramescu, S. *Environ. Technol.* **2004**, *25*, 1131−1141.
(24) Vohra, M. S.; Selimuzzaman, S. M.; Al-Suwaiyan, M. S. *Int. J. Environ. Res.* **2011**, *5*, 247−254.
(25) Vohra, M. S. *Fresenius Environ. Bull.* **2011**, *20*, 1308−1313.
(26) Rorke, G. V.; Mühlbauer, R. M. *Process Met.* **1999**, *9*, 731−740.
(27) Grigor'eva, N. V.; Smirnova, Y. V.; Dulov, L. E. *Microbiology* **2009**, *78*, 402−406.
(28) Kita, Y.; Takada, T.; Mihara, S.; Whelan, B. A.; Tohma, H. *J. Org. Chem.* **1995**, *60*, 7144−7148.
(29) Yadav, J. S.; Reddy, B. V. S.; Shubashree, S.; Sadashiv, K. *Tetrahedron Lett.* **2004**, *45*, 2951−2954.
(30) Wu, G.; Liu, Q.; Shen, Y.; Wu, W.; Wu, L. *Tetrahedron Lett.* **2005**, *46*, 5831−5834.
(31) Prakash, O.; Kaur, H.; Batra, H.; Rani, N.; Singh, S. P.; Moriarty, R. M. *J. Org. Chem.* **2001**, *66*, 2019−2023.
(32) Wu, G.; Wu, W.; Li, R.; Shen, Y.; Wu, L. *Chem. Lett.* **2007**, *36*, 188−189.

(33) Anil Kumar, M.; Reddy, K. R. K. K.; Reddy, M. V.; Reddy, C. S.; Reddy, C. D. *Synth. Commun.* **2008**, *38*, 2089−2095.
(34) Lente, G.; Kalmár, J.; Baranyai, Z.; Kun, A.; Kék, I.; Bajusz, D.; Takács, M.; Veres, L.; Fábián, I. *Inorg. Chem.* **2009**, *48*, 1763−1773.
(35) Bellér, G.; Bátki, G.; Lente, G.; Fábián, I. *J. Coord. Chem.* **2010**, *63*, 2586−2597.
(36) Smith, R. H.; Wilson, I. R. *Aust. J. Chem.* **1966**, *19*, 1357−1363.
(37) Smith, R. H.; Wilson, I. R. *Aust. J. Chem.* **1966**, *19*, 1365−1375.
(38) Smith, R. H.; Wilson, I. R. *Aust. J. Chem.* **1967**, *20*, 1353−1366.
(39) Nagy, P.; Lemma, K.; Ashby, M. T. *Inorg. Chem.* **2007**, *46*, 285−292.
(40) Covington, A. K.; Bates, R. G.; Durst, R. A. *Pure Appl. Chem.* **1983**, *55*, 1467−1476.
(41) Tonomura, B.; Nakatani, H.; Ohnishi, M.; Yamaguchi-Ito, J.; Hiromi, K. *Anal. Biochem.* **1978**, *84*, 370.
(42) *SCIENTIST*, version 2.0; Micromath Software: Salt Lake City, UT, 1995.
(43) Peintler, G. *ZiTa: A comprehensive program package for fitting parameters of chemical reaction mechanisms*, version 4.1; Institute of Chemistry JATE: Szeged, Hungary, 1997. The first use of this program was described in: Peintler, G.; Nagypal, I.; Epstein, I. R. *J. Phys. Chem.* **1990**, *94*, 2954.
(44) Hindmarsh, A. C. *GEAR: Ordinary Differential Equation SolVer*, revision 2; Lawrence Livermore Laboratory: Livermore, CA, 1972.
(45) Nagy, P.; Wang, X.; Lemma, K.; Ashby, M. T. *J. Am. Chem. Soc.* **2007**, *129*, 15756−15757.
(46) Peintler, G.; Nagypál, I.; Jancsó, A.; Epstein, I. R.; Kustin, K. *J. Phys. Chem. A* **1997**, *101*, 8013.
(47) Peintler, G.; Nagypál, I.; Epstein, I. R.; Kustin, K. *J. Phys. Chem. A* **2002**, *106*, 3899.
(48) Nagy, P.; Alguindigue, S. S.; Ashby, M. T. *Biochemistry* **2006**, *45*, 12610−12616.
(49) Espenson, J. H. *Chemical Kinetics and Reaction Mechanisms*, 2nd ed.; McGraw-Hill Series in Advanced Chemistry; McGraw-Hill Inc.: New York, 1995; pp 49−52.
(50) SO_4^{2-} is in excess over SO_5^{2-} even in Oxone, which is used as the SO_5^{2-} source.
(51) $SCN^- + 2OH^- \rightarrow OSCN^- + H_2O + 2e^-$ ($\varepsilon = -0.44$ V at pH ≈ 7).[5] $HSO_5^- + 2e^- \rightarrow SO_4^{2-} + OH^-$ ($\varepsilon = +1.44$ V at pH ≈ 7).[34]
(52) Barnett, J. J.; McKee, M. L.; Stanbury, D. M. *Inorg. Chem.* **2004**, *43*, 5021−5033.
(53) Lemma, K.; Ashby, M. T. *Chem. Res. Toxicol.* **2009**, *22*, 1622.
(54) Reijenga, J. C.; Gagliardi, L. G.; Kenndler, E. *J. Chromatogr. A* **2007**, *1155*, 142−145.
(55) Lente, G.; Fábián, I.; Poë, A. J. *New J. Chem.* **2005**, *29*, 759−760.
(56) Stanbury, D. M. *Adv. Inorg. Chem.* **1989**, *33*, 69−138.